



Published in final edited form as:

*Biomed Mater.* ; 13(4): 045005. doi:10.1088/1748-605X/aab66f.

## Biofabrication of Injectable Fibrin Microtissues for Minimally-Invasive Therapies: Application of Surfactants

Ramkumar Annamalai<sup>#</sup>, Tapan Naik<sup>#</sup>, Haley Prout<sup>#</sup>, Andrew J. Putnam, and Jan P. Stegemann<sup>\*</sup>

Department of Biomedical Engineering, University of Michigan, Ann Arbor MI

### Abstract

Microtissues created from the protein fibrin and containing embedded cells can be used in modular tissue engineering approaches to create larger, hierarchical and complex tissue structures. In this paper we demonstrate an emulsification-based method for the production of such fibrin microtissues containing fibroblasts and endothelial cells and designed to promote tissue vascularization. Surfactants can be beneficial in the microtissue fabrication process to reduce aggregation and to facilitate recovery of microtissues from the emulsion, thereby increasing yield. The nonionic surfactants Pluronic L101® and Tween 20® both increased microtissue yield in a dose-dependent fashion. Cell viability of both human fibroblasts and human endothelial cells remained high after exposure to low surfactant concentrations but decreased with increasing surfactant concentration. L101 was markedly less cytotoxic than Tween, and therefore was the surfactant of choice in this application. The yield of cell-laden microtissues increased with increasing L101 concentration, though microtissues were slightly larger at low concentrations. The total metabolic activity of cells in retrieved microtissues was bimodal and was highest at an L101 concentration of 0.10 % wt/vol. Network formation by endothelial cells in microtissues embedded in surrounding 3D fibrin hydrogels was also most extensive in microtissues made using an L101 concentration of 0.10 % wt/vol. Minimally-invasive delivery of microtissue populations was demonstrated by injection through a standard 18G needle, and the ability to form robust endothelial networks was maintained in injected microtissue populations. Taken together, these data demonstrate a facile emulsification-based method to create modular, cell-laden hydrogel microtissues that can be delivered by injection to promote tissue regeneration. Appropriate selection of the type and concentration of surfactant used in the process can be used to maximize viability and specialized function of the embedded cells. Such biomaterial-based microtissues may have broad applicability in cell-based therapies and tissue engineering.

### Keywords

Surfactants; fibrin; microtissues; emulsification; microemulsion; minimally-invasive therapy

<sup>\*</sup>Corresponding Author: Jan P. Stegemann, Department of Biomedical Engineering, University of Michigan, 1101 Beal Ave., Ann Arbor, MI 48109, Tel: 734-764-8313, Fax: 734-647-4834, jpsteg@umich.edu.

<sup>#</sup>These authors contributed equally

## Introduction

Directed assembly of cell-laden, microscale modules to create larger hierarchical tissue structures is an approach to biofabrication with many potential applications [1]. In particular, this approach enables the assembly of complex tissue architectures in clinically-relevant shapes and sizes. Also, cell-laden tissue modules can be used to efficiently maintain highly metabolic cells in perfusion bioreactors [2, 3], to develop injectable cell [4–6] and drug [7, 8] delivery systems, and to fabricate high throughput in vitro drug testing assays [9]. Material-free modules (e.g., cell aggregates) have had some success [10], but matrix-based modules have the advantage that they have enhanced space-filling capacity and can more readily remodel into mature macrotissues [11]. Critical enabling features of the modular strategy include the ability to circumvent diffusion limitations, recreate tissue-specific microarchitecture, and to provide control over cell and matrix distribution [12]. Further, it represents a scalable strategy that can also be integrated with traditional approaches to enhance their functionality [13]. Various enabling technologies to improve module biofabrication have been proposed, including molds, microfabrication, and microfluidic techniques. However, a key determinant of the success of the modular approach is the robustness and efficiency of the process used to create the discrete, modular microtissues.

Fibrinogen is a key protein in the coagulation cascade that undergoes thrombin-mediated polymerization to form an insoluble fibrin matrix following injury [14]. Fibrin matrices play a major role in hemostasis and subsequently also serve as a scaffold for tissue repair. The fibrin network supports the infiltration and differentiation of various cell types, including endothelial cells and fibroblasts, which are involved in tissue regeneration. In addition, smaller peptides released upon the degradation of fibrin matrices serve as chemokines for reparative cells [15]. Fibrin is therefore often used as a material in regenerative medicine because it is a natural matrix that is rich in bioactive signals, and which can provide cues for directing cell function. Additionally, fibrin materials have the advantage that they can be easily manipulated to modify their porosity, fiber thickness, mechanical properties [16, 17], and polymerization kinetics [18]. The ease of handling, control over polymerization, and potent bioactivity make fibrin an attractive material for use in tissue biofabrication strategies.

Agitation-based emulsification is an efficient and facile way to create aqueous protein or polymeric droplets via phase separation in an oil/lipophile phase. Cells, proteins, and/or biomolecules can be included in these droplets by suspending them in the aqueous phase prior to dispersion, and subsequent gelation of the suspending hydrogel matrix/polymer yields composite modular microtissues with entrapped cells, which can be collected from the oil phase [7, 19–21]. Such emulsions are kinetically stable initially but can agglomerate over time due to thermodynamic instability [22]. The result can be aggregation and clumping of hydrogel microtissues, which negatively affects the recovery and overall yield during separation from the oil phase. For this reason, amphiphilic surfactants are often added to such emulsions to increase thermodynamic stability and promote dispersion, and thereby facilitate recovery of individual microtissues. Although many surfactants offer cytoprotection [23, 24], they can also interfere with the lipid bilayer of the cell membrane [25, 26] and thereby affect cell function and viability. Therefore, optimizing surfactant concentration is an essential component of biofabricating microtissues via emulsion.

Surfactants used in biotechnology are typically selected for their relatively high biocompatibility and low cytotoxicity. Pluronic® L101 is a block copolymer consisting of hydrophobic ethylene oxide moieties and hydrophilic propylene oxide moieties [26] that has been used in biotechnology and pharmaceutical applications including for controlled drug delivery [27] and as an immunological adjuvant [28]. Tween® 20 (also called Polysorbate 20) is another nonionic surfactant that contains sorbitan monolaurate as a hydrophobic component and polyoxyethylene on the hydrophilic end [29], which has been commonly used in formulating therapeutic monoclonal antibodies [30, 31] due to its biocompatibility and good stabilizing properties for proteins. These surfactants differ in their hydrophilic-lipophilic balance (HLB). L101 has an HLB in the range of 1–7 reflecting its larger hydrophobic portion, whereas Tween has an HLB around 17 because of its larger hydrophilic component [32]. Both of these surfactants can form micelles in an aqueous environment above a concentration threshold known as critical micelle concentration (CMC). The HLB and CMC of a surfactant are critical determinants of their properties, including cytotoxicity [33].

In the present study, discrete fibrin microtissues were fabricated using a facile water-in-oil emulsification method (Fig. 1A). These microtissues were designed to promote the formation of new blood vessels (vasculogenesis) within the fibrin matrix, such that when populations of microtissues are delivered to a site of injury, new blood vessel networks can form rapidly (Fig. 1B). The tissue modules contained both human endothelial cells (EC) and human fibroblast cells (FB), since this cell combination leads to the robust formation of vessel networks in 3D matrices [6]. Importantly, the modular approach allows minimally invasive delivery of the microtissues as an injectable paste. To increase the yield of viable and functional vasculogenic microtissues, we investigated the use of biocompatible surfactants to prevent aggregation of discrete modules and to facilitate collection from the oil phase. The effects of surfactants on microtissue size and yield were investigated. Similarly, processing effects on cell viability, metabolic activity, and the ability to initiate vasculogenesis were assessed. Finally, the ability of biofabricated microtissue populations to be delivered by injection and to form interconnected vessel networks over time in 3D culture was validated. These studies elucidate the effects of surfactants on the processing and recovery of modular protein microtissues and demonstrate their utility in improving the yield of functional modules for tissue regeneration.

## Materials and Methods

### Biopolymers and cell culture

Bovine plasma fibrinogen (Sigma, St. Louis, MO) with a molecular weight of 137 kDa and 75% clottable protein was used. A fibrinogen stock solution of 4.0 mg/mL clottable protein was made by dissolving lyophilized fibrinogen in serum-free culture media at 37 °C. For cell culture experiments, the fibrinogen stock solution was filter-sterilized using 0.22 µm low-protein-binding poly(ether sulfone) (PES) membrane filters (Millex, Billerica, MA). Thrombin from bovine plasma (Sigma) with a stock concentration of 50 U/mL was used to make fibrin hydrogels and fibrin microtissues.

Human umbilical vein endothelial cells (EC, passage 5–8) and normal human lung fibroblasts (FB, passage 9–12) were obtained from a commercial source (Lonza Inc., Walkersville, MD). Cells were expanded in tissue culture flasks and maintained in standard cell culture incubators. EC were culture-expanded in EGM-2 media (Lonza) as per the manufacturer's guidelines. FB were cultured with DMEM-Glutamax (Gibco) supplemented with 10% fetal bovine serum (FBS, Gibco) and 1% penicillin-streptomycin (Gibco). For co-culture studies, EGM-2 media was supplied for both cell lineages.

### Biofabrication of modular microtissues and bulk gels

Fibrin microtissues and bulk gels were prepared as described previously [4, 6]. Briefly, 1.0 mL of fibrin hydrogel solution was made by mixing 625  $\mu$ L fibrinogen, 100  $\mu$ L FBS, 20  $\mu$ L thrombin, and 255  $\mu$ L of cell suspension containing  $0.25 \times 10^6$  endothelial cells and  $0.25 \times 10^6$  fibroblast cells (1:1 ratio). For fabricating fibrin microtissues, the well-mixed cell-matrix suspension was quickly dispensed into a stirred polydimethylsiloxane (PDMS, 100 cS; Clearco, Bensalem, PA) solution kept at on ice and allowed to emulsify for 5 min. The temperature of the bath was then increased to 37 °C to facilitate gelation of the emulsified fibrin microtissues, and mixing was continued for an additional 25 min. The impeller speed was kept at 600 rpm throughout the process. The fibrin microtissues were then collected by centrifuging the resulting microemulsion at 200 g for 5 min and washing twice with surfactant-containing solutions in PBS. The collected microtissues were then maintained in suitable culture media. For the vessel sprouting assay, the microtissues were embedded in a larger fibrin bulk gels with the same composition as described above.

Bulk fibrin gels were made in 24-well plates (1.9 cm<sup>2</sup> per well) for studying cytotoxicity of surfactants on EC and FB. After dispensing the hydrogel solution, the 24-well plate was incubated in 37 °C for 30 min to facilitate gelation. After gelation, complete media was added and left overnight in the incubator.

The injectability of the microtissues was tested by delivery through an 18-gauge needle. The microtissue suspension was aspirated into a 1 mL syringe and then dispensed at a rate of 0.5 mL/sec through an 18-gauge needle. The quality of the dispensed microtissues was then analyzed using the cell viability and endothelial sprouting assays.

### Surfactant treatments and microtissue recovery

Solutions with selected concentrations (0.01%, 0.1%, 1% v/v) of Pluronic® L101 (denoted as L101, BASF, Milford, CT) and Tween® 20 (denoted as Tween, Sigma) were made in sterile Hank's balanced salt solution (HBSS, Gibco). For initial cytotoxicity analysis, fibrin hydrogels containing EC and FB were treated with one mL of surfactant solution per 0.5 mL hydrogel at defined concentrations for 90 min. The treatment timeframe was selected based on the time taken for the microtissue fabrication process during which the cells are exposed to surfactants. Control samples were treated with pure HBSS solution. After the 90 min incubation period, bulk gels were washed three times in PBS and replenished with complete culture media. The viability and metabolic activity of EC and FB were studied separately after 1-hour and 24-hour culture periods.

Microtissue recovery using different surfactants was assessed by preparing 5 mL of surfactant solution at 0.01%, 0.1%, and 1% surfactant in HBSS and adding this solution to 40 mL of hydrogel-PDMS emulsion. The resulting preparations were mixed well for 5 min by gentle inversion to separate microtissues from PDMS. The solution was then centrifuged at 200 g for 5 min. After centrifugation, the supernatant PDMS phase was removed without disturbing the bottom aqueous phase. Microtissues were then transferred to new centrifuge tubes and washed with 5 ml of the surfactant solution, and centrifuged at 200 g for 5 min two more times. After the final centrifugation, microtissues were suspended in culture media and maintained at 37 °C until ready for use. The total microtissue yield and size after each treatment were quantified through image analysis. Briefly, after the final wash, the microtissues were suspended in 1 mL of PBS. A small quantify of the suspension (50 µL) was sampled (n=3) and dispensed between two glass coverslips separated by 0.5 mm-thick spacers. Phase contrast image of the full droplet was taken using inverted microscope (Nikon), and the total number and the size of the microtissues were manually quantified through Fiji (ImageJ) software (National Institutes of Health).

### Cell viability and metabolic activity

Cell viability and metabolic activity were assayed at 1 hour and 24 hours after fabrication of microtissues and bulk gels. Ethidium homodimer (Invitrogen, Grand Island, NY) and calcein-AM (Live/Dead®, Invitrogen) were used for vital staining. Briefly, a working solution containing 1 µM calcein-AM and 2 µM ethidium homodimer was prepared, and samples were incubated in the working solution for 30 minutes. After two washes in 10 mM PBS, fluorescent images of the fibrin hydrogel and microtissues (20 µL suspension) were taken using appropriate filters (excitation/emission 488/520 for calcein-AM, 528/617 for ethidium homodimer). For viability quantification, the total number of live and dead cells were counted manually using Fiji (ImageJ) software. All treatments were done in triplicates, and a minimum of 3 images per sample was used for the analysis. Percent viability was calculated using the formula: percent viability = (total number of live cells × 100/total number of cells dead or alive). For measuring metabolic activity, 50 µL of the Prestoblue stock solution was added to 450 µL of microtissues suspension or in the case of bulk gels, the stock solution was added to the 450 µL of media on top of the gel and incubated at 37°C for 30 min. After the incubation period, the solution was transferred to a 96 well plate, and fluorescence readings (excitation/emission 560/610) were taken using a microplate reader. The obtained data are presented in arbitrary fluorescence units (FLU).

### Quantification of endothelial sprouting

The ability of the endothelial cells in the fabricated microtissues to form vessel sprouts was tested by embedding them in a 3D fibrin hydrogel matrix. For easy detection of microtissues after embedding, microtissues were coated with fluorescently-labeled fibrinogen by incubating them in 5 µg/ml of FITC-fibrinogen (Sigma) staining solution for 10 min. The stained microtissues were washed twice in PBS, mixed with the hydrogel solution, and microtissue-containing hydrogels were cast in 24-well tissue culture plates. After complete gelation, 1 ml of EGM-2 media was supplied for each 500 µL gel and maintained at 37°C in an incubator. Samples were collected at day 7 and 14, fixed in a 10 % formalin solution (Z-Fix) for 30 min and stained with rhodamine-labeled endothelial cell-specific marker Ulex

Europaeus Agglutinin I (UEA-I, Vector Laboratories, Burlingame, CA). DAPI (Invitrogen) was used as nuclear counter-stain. Fluorescent images were captured with an inverted fluorescence microscope (Nikon). Sprout lengths were quantified manually through image analysis using Fiji (Image J) software as described previously [6]. Entire well was imaged for quantification whenever possible. At least 3 samples per condition and 3 images per sample were used for quantification.

## Statistical Analysis

All measurements were performed at least in triplicate. Data are plotted as means with error bars representing the standard error of the mean. Two-way ANOVA was used for multi-group comparisons, and Student's *t*-test with a 95% confidence limit (two-tailed and unequal variance) was used for paired comparisons and the *p*-values adjusted with Bonferroni correction wherever applicable. Differences with *p* < 0.05 were considered statistically significant.

## Results and Discussion

### Effect of surfactant concentration on microtissue yield

L101 and Tween are both commonly used in biotechnology applications and were therefore used in this study in an effort to stabilize the emulsions and enhance microtissue recovery. In the microtissue fabrication process, solutions of surfactant dissolved in PBS were gently mixed into the PDMS-microtissue emulsion, followed by centrifugation to promote the transfer of the microtissues to the aqueous PBS-surfactant phase. The surfactant solutions were also used to wash the microtissues after collection to remove any remaining PDMS. Figure 2 shows the yield of acellular fibrin microtissues as a function of surfactant concentration for both L101 and Tween. Final microtissue yield increased in a dose-dependent fashion with surfactant concentration for both surfactant types (*p*<0.01). However, there was no statistically significant difference in the yield between surfactant types. It was also noted that increasing surfactant concentration markedly decreased the degree of microtissue aggregation during the wash steps.

The increase in microtissue yield can be attributed to an inhibition of aggregation as well as a lowering of the surface tension between the aqueous and lipophilic phases. When a surfactant is mixed into the emulsion, the surfactant molecules preferentially localize to the water-lipophile interface, which is thermodynamically favorable for amphiphiles [22]. In the case of the microtissues, this has the effect of preventing aggregation and stabilizing the emulsion by lowering the free energy of the system, as represented by:

$$\Delta G_f = \gamma \Delta A - T \Delta S,$$

Where  $G_f$  is the free energy of formation of the microemulsion,  $\gamma$  is the surface tension of the water-lipophile interface,  $A$  is the surface area of the interface,  $T$  is the temperature, and  $S$  is the change in entropy. During emulsification, the aqueous phase is broken down into small droplets by the impeller, which increases the surface area ( $\Delta A$ ) and entropy ( $\Delta S$ ) of the system. To be thermodynamically stable, the free energy ( $G_f$ ) must be kept low.



Localization of surfactant at the water-lipophile interface dramatically decreases the surface tension ( $\gamma$ ) and therefore stabilizes the system by lowering the free energy. Stable emulsions are less likely to aggregate, which enhances recovery of individual microtissues. Also, the reduced surface tension facilitates the transfer of the hydrogel microtissues into the aqueous phase, which further increased yield.

### Effect of surfactants on cell viability in 3D fibrin matrices

Although surfactants exhibit membrane protective function, at high concentrations, they can disrupt the lipid bilayer of mammalian cells and thereby impact their function and viability. For this reason, relatively low concentrations of surfactant were used in this study. However, assessment of cell viability and function after surfactant treatment is still critical to validate the use of a particular surfactant. Figure 3 shows the viability of FB and EC at day 1 after embedding the cells in 3D fibrin matrices that were incubated with surfactant solutions for 90 min before washing and subsequent culture. Fibroblast viability (Fig. 3A, 3B) was not different from control at 0.01% and 0.1% L101 but was dramatically reduced when exposed to 1.0% L101 ( $p < 0.05$ ). Tween significantly decreased FB viability at 0.1% ( $p < 0.05$ ), and there were very few live cells observed at 1.0% ( $p < 0.001$ ). Endothelial cell viability (Fig. 3C, 3D) showed a similar trend, with no significant difference from control at the lower concentrations of L101, but a very marked reduction in viability when exposed to 1.0% L101 ( $p < 0.001$ ). Both 0.1% and 1.0% concentrations of Tween caused deduced endothelial cell viability, relative to control ( $p < 0.05$ ). These results suggest that L101 is less damaging to mammalian cells than Tween at these concentrations.

The difference in cytotoxicity between surfactants is mainly due to the difference in hydrophilic-lipophilic balance. Generally, surfactants with low HLB (3–6) are preferred for water-in-oil microemulsions, whereas surfactants with higher HLB (8–18) are used for oil-in-water systems [22]. The critical packing parameter (CPP) is a measure of the preferred geometry adopted by a surfactant at a water-lipophile interface [34]:

$$CPP = \frac{v}{a * l_c}$$

Where  $v$  is the partial molar volume of the hydrophobic end of the surfactant molecule,  $a$  is the area of the hydrophilic head group, and  $l_c$  is the length of the lipophilic tail. Surfactant molecules typically have a conical shape that varies the HLB. In low HLB surfactants, the molecule tapers toward the hydrophilic end because of the relatively large lipophilic head group, resulting in a high CPP. Conversely, in high HLB surfactants, the large hydrophilic head group leads to a taper toward the lipophilic end and a lower CPP. For this reason, high HLP (and consequently low CPP) surfactants tend to penetrate cell membranes more efficiently and therefore tend to have more pronounced effects on cell function. In the current study, we observed this effect since Tween has a higher HLB than L101, and consequently had a more marked adverse effect on cell viability in 3D fibrin matrices. For this reason, subsequent studies were carried out using only L101, which has a lower HLB and consequently less detrimental effects on cell viability.

### Effects of surfactant on cell-seeded fibrin microtissues

The effects of L101 surfactant on EC-FB-seeded fibrin microtissues was further investigated using additional, intermediate surfactant concentrations (0.20% and 0.40%). Figure 4 shows the yield and the average diameter of cell-seeded microtissues as a function of L101 concentration. As in the acellular fibrin microtissue studies, increasing surfactant concentration had a direct and dose-dependent positive effect on microtissue yield (Fig. 4A). The effect of surfactant concentration on microtissue size was not strong, though microtissues made at 0.01% L101 were significantly larger than those made at higher surfactant concentrations (Fig. 4B). It should be noted that the surfactant solution is added after the microtissues have already gelled in the emulsion. Therefore any change in size is likely due to aggregation and/or preferential recovery of larger microtissues. However, microtissue size can be varied in this fabrication process by controlling emulsification conditions such as impeller geometry, impeller speed, and the viscosity of the lipophilic phase [35, 36].

The effects of L101 concentration on cell viability and function in fibrin microtissues are shown in Figure 5. Cell viability and metabolic activity were measured at 1 hour post-fabrication to assess the effect of microtissue emulsification and processing, and again at 24 hours post-fabrication to determine longer-term effects. Initial total cell viability (Fig. 5A) was not affected at low L101 concentrations (0.01%, 0.1%, 0.2%), but at higher concentrations (0.4%, 1.0%) there was a significant reduction in viability ( $p < 0.05$ ). The observed effects were similar at the longer time point, though in this case the 0.2% treatment also exhibited decreased viability compared to the 0.1% treatment. Metabolic activity, as measured by mitochondrial reduction of a resazurin dye (Fig. 5B), of cells in microtissue populations was not significantly different at the 1 hour time point, except that activity was lower at the 0.01% concentration. At the 24 hour time point, both the 0.1% and 0.2% L101 concentrations resulted in the increased metabolic activity of microtissue populations, which dropped off very significantly at higher L101 concentrations, in concert with the reduction in cell viability. In all conditions, microtissues were intact, and cells could be visualized inside the microtissue matrix (Fig. 5C), and these observations validated the viability assessment. It should be noted that the metabolic characterization of microtissue populations depends on the number of microtissues, the viability of the embedded cells, and their mitochondrial activity. It is likely that reduced metabolic activity at lower L101 concentrations is due to a decrease in microtissue yield. However, at higher L101 concentrations, which give high yields, reductions in metabolic activity are likely caused by a decreased number of cells and/or delayed effects of surfactants [26].

### Effect of surfactant concentration on endothelial network formation

The microtissues in this study were designed as delivery vehicles for EC and FB, as a method to promote rapid revascularization in ischemic tissues. Therefore, the ability of microtissues to form vascular networks was assessed by embedding EC-FB-seeded microtissues into surrounding acellular fibrin hydrogels. To differentiate the embedded microtissues from the surrounding gel, the microtissues were labeled by coating with FITC-fibrinogen, while the surrounding gel was unlabeled. Figure 6A shows images of endothelial networks produced by microtissues after 14 days of embedding. Microtissues made with



0.01% L101 showed robust sprouting in a radial pattern from clumps of microbeads. Microtissues made with 0.1% L101 also showed vigorous development of an endothelial network, and microtissues were more evenly distributed throughout the surrounding matrix. Vessel network formation was markedly reduced in 0.2% L101 samples and was essentially completely abrogated in microtissues made with 1.0% L101, presumably reflecting the reduced viability and metabolic activity in these samples, and in spite of the larger yield of these microtissues. Quantification of the total network length produced in the fibrin matrix (Fig. 6B) showed that samples made with 0.1% L101 generated significantly longer vessel networks ( $p < 0.05$ ), compared to the other conditions. This finding demonstrates the importance of both preventing aggregation of microtissues and maintaining cell viability to achieve robust and widespread vascularization.

### Injectability of microtissues

To demonstrate the potential of modular fibrin microtissues as a minimally invasive method to deliver a vascularization therapy, populations of microtissues made with 0.1% L101 were aspirated into a standard syringe and then injected through a 18G needle at 0.5 mL/min and maintained in suspension culture tubes (Fig. 7A). The viability of cells in the injected microtissues was then assessed at 1 hour and 24 hours after injection and was compared to controls transferred to the culture tube using a standard pipette. Cell viability (Fig. 7B) was high and not significantly different between injected and control samples at both time points. Visualization of the microtissues and the embedded cells (Fig. 7C) similarly found no differences between injected and controls.

Injected and control microtissues were also embedded in acellular surrounding hydrogels to characterize vessel network formation. By day 14 in culture, both samples showed robust endothelial sprouting and interconnected vessel networks (Fig. 8A), and the network was well-distributed in the surrounding matrix. Quantification of the total network length (Fig. 8B) showed no statistically significant difference between injected and control microtissues ( $p < 0.05$ ). These results indicate that microtissues can be delivered via injection without compromising cell viability or functionality, an essential requirement for developing minimally invasive cell-based therapies. The modular microtissue format has the advantage that cells are embedded in a surrounding protective matrix, which allows injection, promotes engraftment, and can be tailored to enhance desired cellular functions. Minimally invasive strategies are promising because they result in smaller wounds, a reduced risk of infection, and more direct host integration. While the field of cell therapy and matrix-assisted cell delivery is still in its infancy, there is a growing enthusiasm that such approaches will provide new treatments for challenging pathologies [37, 38].

### Conclusions

Taken together, these studies show that fabrication of cell-containing microtissues and the overall function of the resulting modules can be improved by careful selection of surfactants. While amphiphilic surfactants have been used widely in biotechnology, their use to stabilize microemulsions of hydrogel materials is still not well understood. Our results show that surfactants can affect the yield of microtissues in a dose-dependent manner, but this benefit

must be balanced with potential effects on cell viability and function. In our study, Tween and L101 had similar beneficial effects on the yield of microtissues seeded with endothelial cells and fibroblasts, but L101 proved to be significantly less cytotoxic based on cell viability, metabolic activity, and the ability to generate robust vascular networks. This effect is potentially due to the relatively low hydrophilic-lipophilic balance and resulting high critical packing parameter of L101, which provides some guidance on selection of surfactants for these applications. Microtissues fabricated using 0.1% L101 showed extensive vessel network formation when embedded in surrounding fibrin hydrogels and could be injected through standard 18G needles without significant loss of function. The modular microtissue format has a wide range of potential applications in cell-based therapeutics and represents an enabling technology in the field of biofabrication, including for the matrix-assisted delivery of cells, enhancement of bioreactors and extracorporeal cell-based devices, the assembly of large and complex tissues, and in the development of bioprinting approaches.

## Acknowledgments

Research reported in this publication was supported in part by the National Heart, Lung, and Blood Institute of the National Institutes of Health under Award Number R01HL118259 (to AJP and JPS) and the National Institute of Arthritis and Musculoskeletal and Skin Diseases under award number R01AR062636 (to JPS). The content is solely the responsibility of the authors and does not necessarily represent the official views of the National Institutes of Health.

## References

1. Jürgen G, et al. Biofabrication: reappraising the definition of an evolving field. *Biofabrication*. 2016; 8(1):013001. [PubMed: 26744832]
2. Tiruvannamalai-Annamalai R, Armant DR, Matthew HWT. A Glycosaminoglycan Based, Modular Tissue Scaffold System for Rapid Assembly of Perfusable, High Cell Density, Engineered Tissues. *PLOS ONE*. 2014; 9(1):e84287. [PubMed: 24465401]
3. McGuigan AP, Sefton MV. Vascularized organoid engineered by modular assembly enables blood perfusion. *Proc Natl Acad Sci U S A*. 2006; 103(31):11461–6. [PubMed: 16864785]
4. Tiruvannamalai Annamalai R, et al. Vascular Network Formation by Human Microvascular Endothelial Cells in Modular Fibrin Microtissues. *ACS Biomaterials Science & Engineering*. 2016; 2(11):1914–1925. [PubMed: 29503863]
5. Tiruvannamalai-Annamalai R, et al. Collagen Type II Enhances Chondrogenic Differentiation in Agarose-based Modular Microtissues. *Cytherapy*. 2016 (In Press).
6. Rioja AY, et al. Endothelial sprouting and network formation in collagen- and fibrin-based modular microbeads. *Acta Biomaterialia*. 2016; 29:33–41. [PubMed: 26481042]
7. Solorio L, et al. Gelatin microspheres crosslinked with genipin for local delivery of growth factors. *J Tissue Eng Regen Med*. 2010; 4(7):514–23. [PubMed: 20872738]
8. Solorio LD, et al. Spatiotemporal Regulation of Chondrogenic Differentiation with Controlled Delivery of Transforming Growth Factor- $\beta$ 1 from Gelatin Microspheres in Mesenchymal Stem Cell Aggregates. *STEM CELLS Translational Medicine*. 2012; 1(8):632–639. [PubMed: 23197869]
9. Au SH, et al. Hepatic organoids for microfluidic drug screening. *Lab Chip*. 2014; 14(17):3290–9. [PubMed: 24984750]
10. Vrij E, et al. Directed Assembly and Development of Material-Free Tissues with Complex Architectures. *Advanced Materials*. 2016; 28(21):4032–4039. [PubMed: 27000493]
11. Urciuolo F, et al. Biophysical properties of dermal building-blocks affect extra cellular matrix assembly in 3D endogenous macro-tissue. *Biofabrication*. 2016; 8(1):015010. [PubMed: 26824879]

12. Nichol JW, Khademhosseini A. Modular Tissue Engineering: Engineering Biological Tissues from the Bottom Up. *Soft matter*. 2009; 5(7):1312–1319. [PubMed: 20179781]
13. Pang Y, et al. Novel integrative methodology for engineering large liver tissue equivalents based on three-dimensional scaffold fabrication and cellular aggregate assembly. *Biofabrication*. 2016; 8(3): 035016. [PubMed: 27579855]
14. Weisel JW, Litvinov RI. Mechanisms of fibrin polymerization and clinical implications. *Blood*. 2013; 121(10):1712–1719. [PubMed: 23305734]
15. Brown AC, Barker TH. Fibrin-based biomaterials: Modulation of macroscopic properties through rational design at the molecular level. *Acta Biomaterialia*. 2014; 10(4):1502–1514. [PubMed: 24056097]
16. Falvo MR, Gorkun OV, Lord ST. The molecular origins of the mechanical properties of fibrin. *Biophysical Chemistry*. 2010; 152(1):15–20. [PubMed: 20888119]
17. Rowe SL, Lee S, Stegemann JP. Influence of thrombin concentration on the mechanical and morphological properties of cell-seeded fibrin hydrogels. *Acta Biomaterialia*. 2007; 3(1):59–67. [PubMed: 17085089]
18. Jiang B, et al. Fibrin-Loaded Porous Poly(Ethylene Glycol) Hydrogels as Scaffold Materials for Vascularized Tissue Formation. *Tissue Engineering Part A*. 2012; 19(1–2):224–234. [PubMed: 23003671]
19. Annamalai RT, et al. Collagen Type II enhances chondrogenic differentiation in agarose-based modular microtissues. *Cytotherapy*. 2016; 18(2):263–277. [PubMed: 26794716]
20. Wise JK, et al. Synergistic enhancement of ectopic bone formation by supplementation of freshly isolated marrow cells with purified MSC in collagen-chitosan hydrogel microbeads. *Connect Tissue Res*. 2016; 57(6):516–525. [PubMed: 26337827]
21. Daley EL, Coleman RM, Stegemann JP. Biomimetic microbeads containing a chondroitin sulfate/chitosan polyelectrolyte complex for cell-based cartilage therapy. *J Mater Chem B Mater Biol Med*. 2015; 3(40):7920–7929. [PubMed: 26693016]
22. Lawrence MJ, Rees GD. Microemulsion-based media as novel drug delivery systems. *Advanced Drug Delivery Reviews*. 2000; 45(1):89–121. [PubMed: 11104900]
23. Cheng CY, et al. Nature of Interactions between PEO-PPO-PEO Triblock Copolymers and Lipid Membranes: (II) Role of Hydration Dynamics Revealed by Dynamic Nuclear Polarization. *Biomacromolecules*. 2012; 13(9):2624–2633. [PubMed: 22808941]
24. Greenebaum B, et al. Poloxamer 188 prevents acute necrosis of adult skeletal muscle cells following high-dose irradiation. *Burns*. 2004; 30(6):539–547. [PubMed: 15302418]
25. Batrakova EV, et al. Mechanism of Pluronic Effect on P-Glycoprotein Efflux System in Blood-Brain Barrier: Contributions of Energy Depletion and Membrane Fluidization. *Journal of Pharmacology and Experimental Therapeutics*. 2001; 299(2):483–493. [PubMed: 11602658]
26. Batrakova EV, Kabanov AV. Pluronic Block Copolymers: Evolution of Drug Delivery Concept from Inert Nanocarriers to Biological Response Modifiers. *Journal of controlled release : official journal of the Controlled Release Society*. 2008; 130(2):98–106. [PubMed: 18534704]
27. Gates KA, et al. A New Bioerodible Polymer Insert for the Controlled Release of Metronidazole. *Pharmaceutical Research*. 1994; 11(11):1605–1609. [PubMed: 7870678]
28. Hunter RL, Bennett B. The adjuvant activity of nonionic block polymer surfactants. II. Antibody formation and inflammation related to the structure of triblock and octablock copolymers. *The Journal of Immunology*. 1984; 133(6):3167–3175. [PubMed: 6491284]
29. Ménard N, et al. Drug solubilization and in vitro toxicity evaluation of lipoamino acid surfactants. *International Journal of Pharmaceutics*. 2012; 423(2):312–320. [PubMed: 22143086]
30. Patapoff TW, Esue O. Polysorbate 20 prevents the precipitation of a monoclonal antibody during shear. *Pharmaceutical Development and Technology*. 2009; 14(6):659–664. [PubMed: 19883255]
31. Tomlinson A, et al. Polysorbate 20 Degradation in Biopharmaceutical Formulations: Quantification of Free Fatty Acids, Characterization of Particulates, and Insights into the Degradation Mechanism. *Molecular Pharmaceutics*. 2015; 12(11):3805–3815. [PubMed: 26419339]
32. Kim C, Hsieh YL. Wetting and absorbency of nonionic surfactant solutions on cotton fabrics. *Colloids and Surfaces A: Physicochemical and Engineering Aspects*. 2001; 187:385–397.

33. Nazari M, Kurdi M, Heerklotz H. Classifying Surfactants with Respect to Their Effect on Lipid Membrane Order. *Biophysical Journal*. 2012; 102(3):498–506. [PubMed: 22325272]
34. Israelachvili J. The science and applications of emulsions — an overview. *Colloids and Surfaces A: Physicochemical and Engineering Aspects*. 1994; 91(Supplement C):1–8.
35. Calabrese, RV., et al. Measurement and analysis of drop size in a batch rotor-stator mixer. 10th European Conference on Mixing; 2000. p. 149-156.
36. Chen HT, Middleman S. Drop size distribution in agitated liquid-liquid systems. *AIChE Journal*. 1967; 13(5):989–995.
37. Pharmaceutical Research and Manufacturers of America. *Medicines in Development: Biologics 2013 report*. Washington, DC: 2013.
38. O’Cearbhaill ED, Ng KS, Karp JM. Emerging medical devices for minimally invasive cell therapy. *Mayo Clin Proc*. 2014; 89(2):259–73. [PubMed: 24485137]

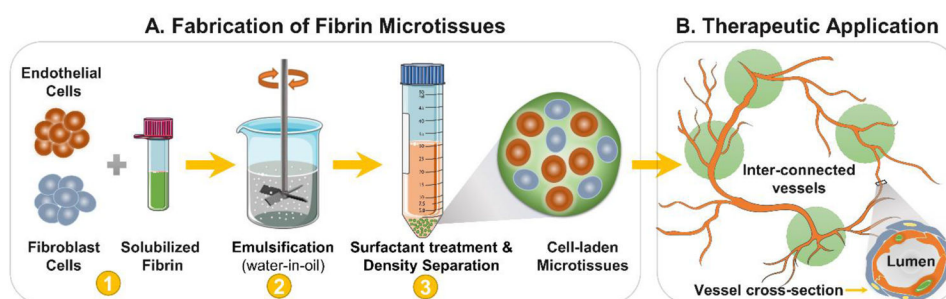


**Figure 1.**

Fabrication of microtissues and application in cell therapy. A) Microtissues were fabricated using a water-in-oil emulsification method as follows: (1) Endothelial cells and fibroblasts were suspended in solubilized fibrin solution and were 2) emulsified in a polydimethylsiloxane bath. 3) Surfactant solution was added to the emulsion, and the microtissues were collected by centrifugation. B) These microtissues are designed to promote the formation of new blood vessels (vasculogenesis) within the fibrin matrix, such that when populations of microtissues are delivered to a site of injury, new blood vessel networks can form rapidly.

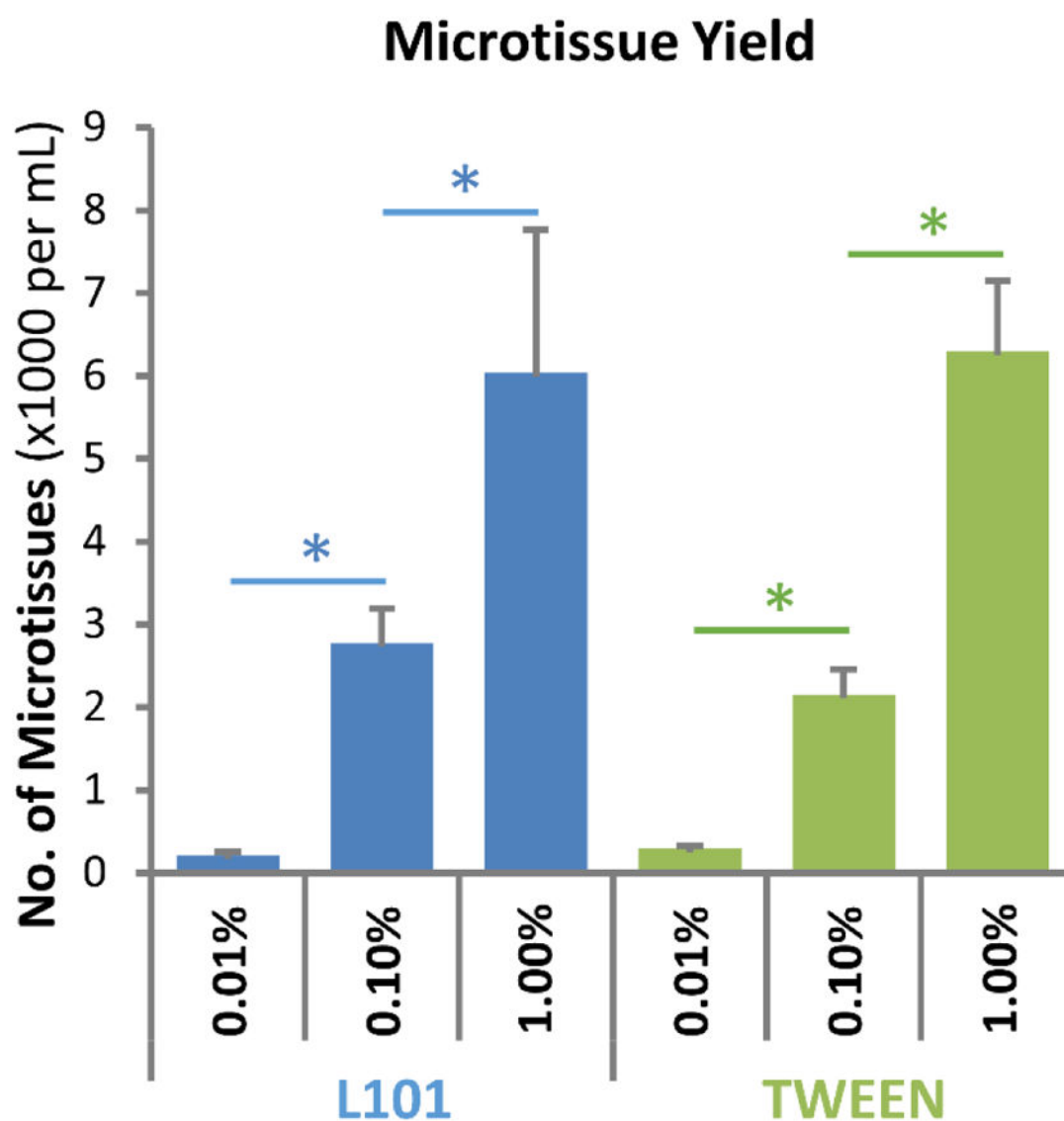


**Figure 2.**

Microtissue recovery after surfactant stabilization. An increase in the concentration of L101 and Tween (0.01–1% v/v) increased the total yield of fibrin microtissues in a dose-dependent fashion ( $p < 0.01$ ). No significant difference in the yield



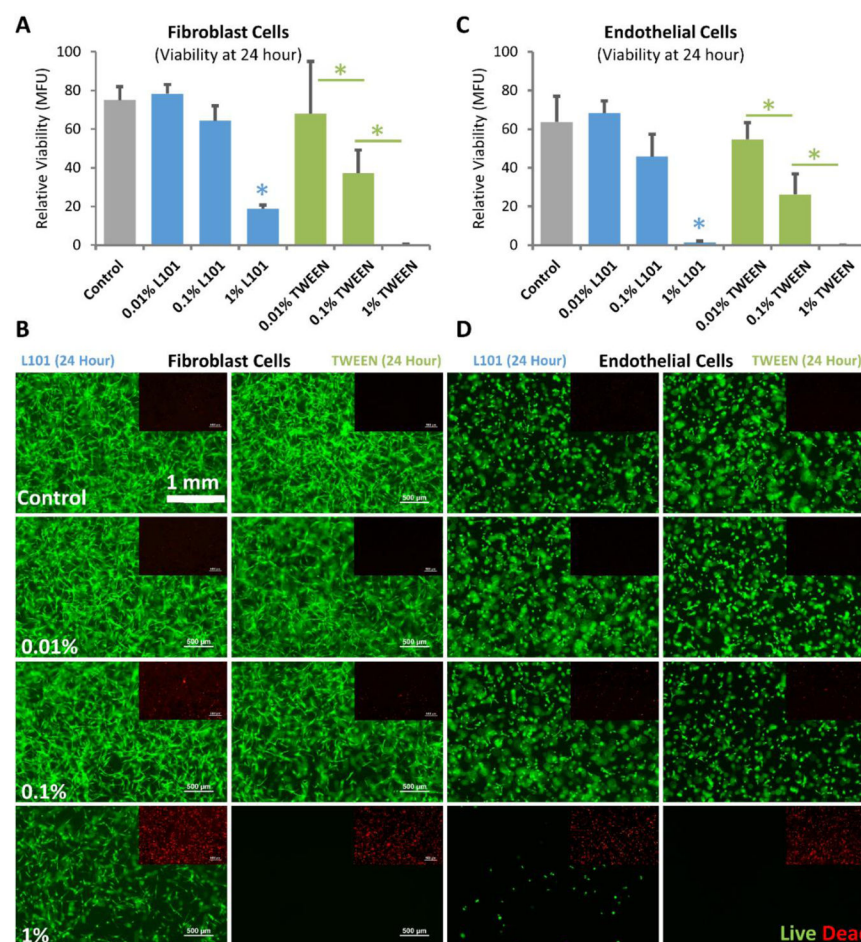


**Figure 3.**

Viability of fibroblasts and endothelial cells embedded in 3D fibrin matrices after surfactant treatment. A) Fibroblast viability as a function of surfactant type and concentration. B) Fluorescent microscopy images of living (green) and dead (inset, red) fibroblasts embedded in surrounding fibrin hydrogels. C) Endothelial cell viability as a function of surfactant type and concentration. D) Fluorescent microscopy images of living (green) and dead (inset, red) endothelial cells embedded in surrounding fibrin hydrogels. Total cell viability was quantified using Live-Dead® assay. \* $p < 0.05$ , \*\* $p < 0.01$ , \*\*\* $p < 0.001$ . MFU = Mean fluorescence units. Scale bar applies to all panels.

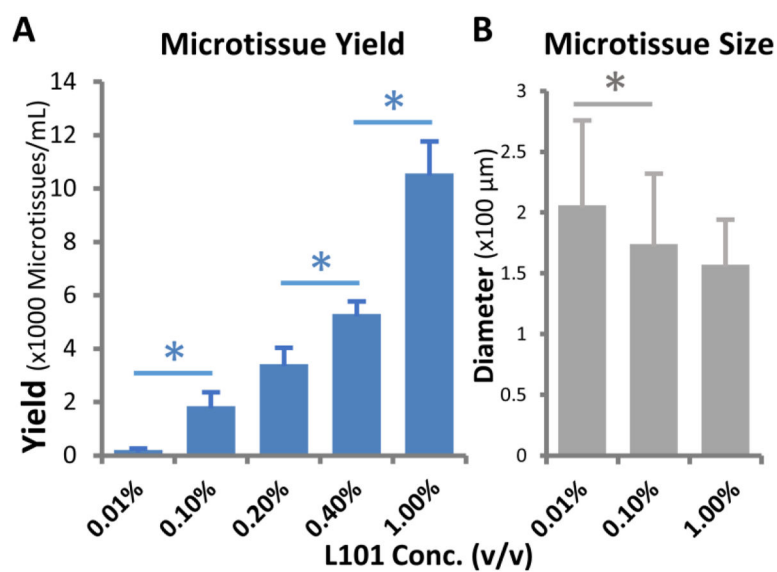


**Figure 4.**

A) Microtissue yield increased with increasing L101 concentration. B) Microtissue diameter as a function of L101 concentration. \* $p < 0.05$ .

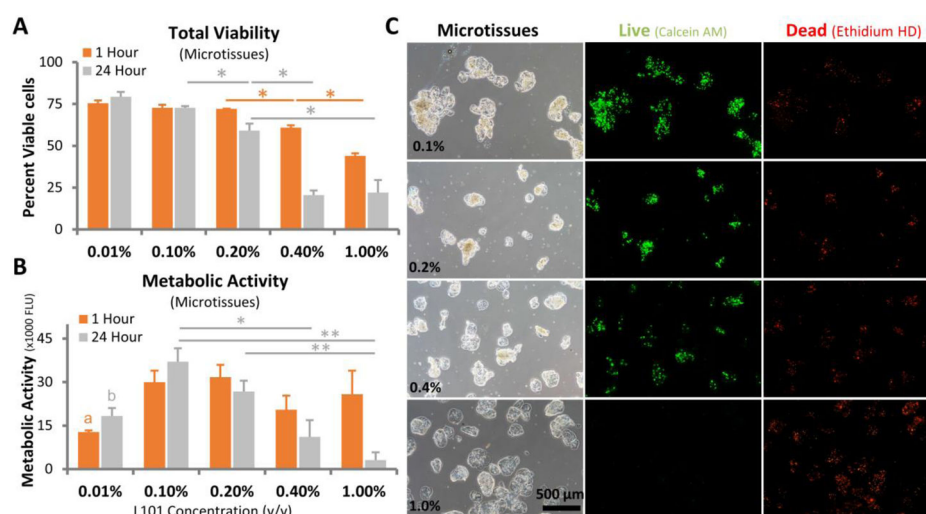


**Figure 5.** Viability and metabolic activity of cells in 3D microtissues. A) Total cell viability in microtissues as a function of L101 concentration at 1 hour and 24 hours post-fabrication. B) Metabolic activity in microtissues as a function of L101 concentration at 1 hour and 24 hours post-fabrication. Metabolic activity presented in arbitrary fluorescence units (FLU). C) Phase contrast and confocal microscopy images of microtissues showing overall morphology and cell viability as a function of L101 concentration at 24 hours post-fabrication. Total cell viability was quantified using Live-Dead® assay, and metabolic activity was measured using Prestoblu® assay \* $p < 0.05$ , \*\* $p < 0.01$ . FLU = arbitrary fluorescence units.

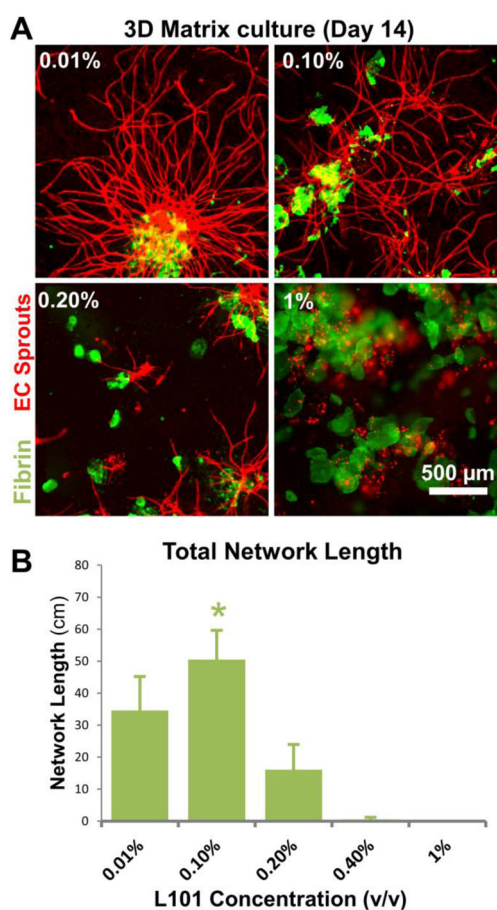


**Figure 6.** Endothelial sprouting from microtissues embedded in surrounding 3D fibrin hydrogels. A) Fluorescent microscopy images of endothelial cell networks (red) sprouting from fibrin microtissues (green) as a function of L101 concentration. B) Total network length of endothelial sprouts in surrounding 3D fibrin hydrogels. \* $p < 0.05$ .

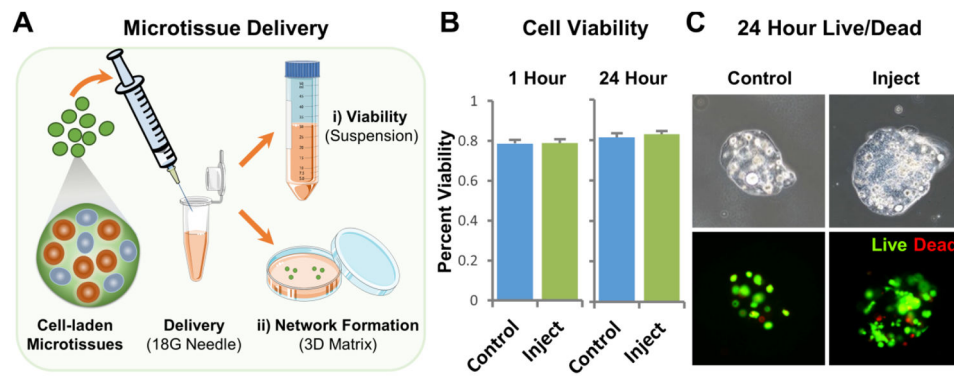


**Figure 7.**

Delivery of microtissues via injection. A) Microtissue populations can be loaded into a standard syringe and delivered via injection through a 18G needle. B) The viability of cells in injected and control microtissues at 1 hour and 24 hours post-fabrication. C) Phase contrast and confocal microscopy images of control and injected microtissues showing overall morphology and cell viability as a function of L101 concentration at 24 hours post-fabrication.

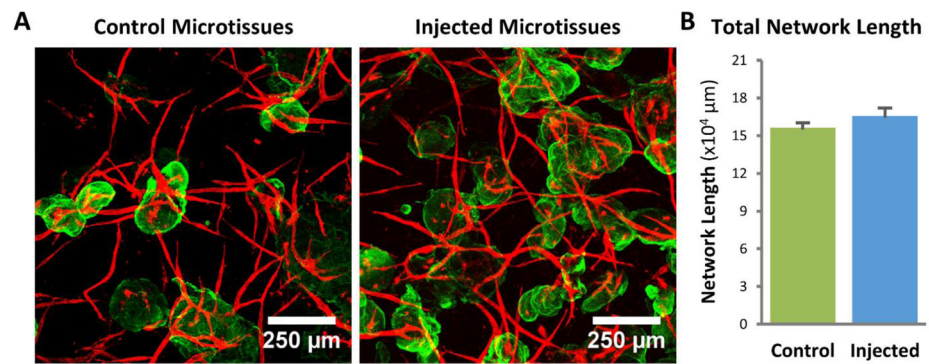


**Figure 8.** Endothelial network formation from microtissues delivered by injection. A) Confocal microscopy images of endothelial cell networks (red) sprouting from fibrin microtissues (green) from control and injected microtissues 14 days after embedding in a surrounding 3D fibrin hydrogel. B) Total network length from control and injected microtissues 14 days after embedding in a surrounding 3D fibrin hydrogel.